Earth and Planetary Science Letters 281 (2009) 188–201

Contents lists available at ScienceDirect

Earth and Planetary Science Letters

journal homepage: www.elsevier.com/locate/epsl

Biogeochemical evidence for euxinic oceans and ecological disturbance presaging the end-Permian mass extinction event

Changqun Cao [a], Gordon D. Love [b,1], Lindsay E. Hays [b], Wei Wang [a], Shuzhong Shen [a], Roger E. Summons [b,*]

[a] State Key Laboratory of Palaeobiology and Stratigraphy, Nanjing Institute of Geology and Palaeontology, Chinese Academy of Sciences, 39 East Beijing Road, Nanjing, Jiangsu, 210008, China
[b] Massachusetts Institute of Technology, Department of Earth, Atmospheric and Planetary Sciences, 77 Massachusetts Avenue, Cambridge MA 02139 USA

ARTICLE INFO

Article history:
Received 16 August 2008
Received in revised form 3 February 2009
Accepted 11 February 2009
Available online 19 March 2009

Editor: M.L. Delaney

Keywords:
Permian Triassic
extinction
Meishan
South China
euxinia
Chlorobiaceae
biomarker hydrocarbons
stable carbon isotopes
strontium

ABSTRACT

The Permian–Triassic Boundary event at 252.2 Ma marks the largest extinction of marine fauna in the Phanerozoic and there is a wide consensus that the extinction coincided with an intense oceanic anoxic event. The stratotype of the Changhsingian Stage, precisely constrained by the PTB Global Stratotype Section and Point (GSSP) and the GSSP for the Wuchiapingian–Changhsingian Boundary, both at Meishan in southern China, is well-documented in respect to geochronology and the pattern of extinction. Here we report secular trends in bulk isotopic parameters and lipid biomarkers in a core spanning 214 m of stratigraphic section across the PTB and through the entire Changhsingian interval. Our analysis of these data, viewed in the context of relative sea level change and strontium isotopes, reveals distinct shifts in paleoenvironmental conditions and profound changes in plankton ecology well before and following the biological extinction event. Specifically, patterns of steroids and triterpenoids indicate a marine plankton community that was heavily dominated by bacteria during the late Wuchiapingian, middle Changhsingian and early Griesbachian stages. Secular trends in aromatic hydrocarbons diagnostic for anoxygenic green sulphur bacteria (Chlorobiaceae) identify periods when euxinic conditions extended into the photic zone during the entire Changhsingian stage. Here also, the $\delta^{15}N$ of organic nitrogen progressively shifted from positive values around +2 or +3‰ to −1‰ coincident with a sharp negative excursion in $\delta^{13}C_{org}$ and slightly postdating the sharp minimum in $\delta^{13}C$ values of inorganic carbon that occurs at the top of Bed 24. These results, together the published chronology indicate that conditions unfavourable for aerobiosis existed in the marine photic zone at Meishan for 1.5 million years prior to the main phase of the biological extinction. The induction of marine euxinic conditions, worldwide, at the end of the Permian was likely a consequence of the aggregation of Pangea and the uplift, weathering and transport of nutrients to the ocean well in advance of the PTB. The protracted and widespread nature of the ensuing oceanic anoxic event suggests a causal association with the mass extinction.

1. Introduction

The Permian–Triassic Boundary (PTB) event culminated at 252.2 Ma with the largest extinction of marine fauna in the Phanerozoic (Raup and Sepkoski, 1982; Erwin, 2006). The pattern of extinction at the Meishan D section with the PTB and Changhsingian-base GSSPs in south China (Yin et al., 2001; Jin et al., 2006), where there are robust geochronological constraints (Bowring et al., 1998; Mundil et al., 2004; Crowley et al., 2006), has been especially well documented (Jin et al., 2000). Further, the main extinction beginning at the base of Bed 25 took place abruptly and, possibly, in as little as 100 kyr (Bowring et al., 1999). The paleontological manifestation of the end-Permian mass extinction is also well known for being accompanied by geochemical evidence for a significant disturbance to ocean chemistry (Holser, 1977). Studies of marine PTB sections worldwide have provided many illustrations of the extinction, marked co-eval negative shifts in the carbon isotopic compositions of carbonates and organic carbon, as well as anomalies in the isotopic compositions of sulfur species (Holser et al., 1989; Faure et al., 1995; Foster et al., 1997; Cao et al., 2002; Sephton et al., 2002; Korte et al., 2004; Newton et al., 2004; Payne et al., 2004; Grice et al., 2005a,b; Berner, 2006; Riccardi et al., 2006; Algeo et al., 2007). At Meishan, $\delta^{13}C$ values for both carbonate and organic carbon show sharp negative spikes coincident with the abrupt faunal change. This study was undertaken to examine the trends in molecular fossils that might provide insight into the biogeochemical processes that accompanied the mass extinction at Meishan.

1.1. Factors underlying the PTB event

There is no consensus on the underlying cause(s) of the PTB event (Benton, 2003; Erwin, 2006). A scenario favoured by many is that the

* Corresponding author.
E-mail address: rsummons@mit.edu (R.E. Summons).
[1] Present address: Department of Earth Sciences, University of California, Riverside, CA 92521, USA.

0012-821X/$ – see front matter © 2009 Elsevier B.V. All rights reserved.
doi:10.1016/j.epsl.2009.02.012

extinction resulted from oceanic and atmospheric disturbances triggered by the eruption of the Siberian flood basalts (Campbell et al., 1992; Kamo et al., 1996; Bowring et al., 1998; Benton, 2003; Kamo et al., 2003; Visscher et al., 2004; Knoll et al., 2007a). In one well-documented variant of this idea, volatiles from the intense volcanism (Visscher et al., 2004) destabilised terrestrial ecosystem leading to unprecedented rates of soil erosion and the transport of the plant debris to the ocean (Visscher et al., 2004; Sephton et al., 2005; Wang and Visscher, 2007). Another scenario, the overturn of a stagnant or anoxic ocean (Isozaki, 1995; Knoll et al., 1996; Wignall and Twitchett, 1996; Isozaki, 1997), is consistent with the concurrence of geochemical anomalies and the selective aspects of mass extinction (Valentine and Jablonski, 1986; Knoll et al., 2007a). C-cycle modelling (Berner, 2006; Payne and Kump, 2007) appears to confirm that multiple factors must be responsible for the magnitude and duration of ^{13}C-anomalies.

Various geological, geochemical, paleoceanographic and biological processes have been explored in an effort to test the linkages between perturbed ocean chemistry, mass extinction and subsequent radiation of organisms. A promising approach towards addressing the problem of the PTB has been to document the physiological attributes of particularly vulnerable and surviving taxa e.g. (Knoll et al., 1996, 2007a). Other researchers (Kump et al., 2005; Riccardi et al., 2006) have specifically proposed that sulfide escaping to the atmosphere during shoaling of the chemocline of a euxinic ocean would provide an effective killing mechanism on land as well as in the marine realm. Regional and global biostratigraphic and chemostratigraphic correlation (Erwin, 1994, 2006) and dramatic improvements in the measurements of the rates of change through isotope geochronology (Bowring et al., 1998; Mundil et al., 2004; Crowley et al., 2006) can help constrain the possible mechanisms behind these geochemical perturbations and their biological consequences.

1.2. Biomarkers as paleoenvironmental and paleobiological indicators at the PTB

Time series of changes in biomarkers provide a window onto the plankton successions and geomicrobiological processes which accompany C- and S-isotopic excursions (Grice et al., 2005a; Sephton et al., 2005; Watson et al., 2005; Xie et al., 2005; Hays et al., 2007; Knoll et al., 2007b; Wang and Visscher, 2007; Wang, 2007). Molecular fossils, in the form of recalcitrant hydrocarbon skeletons of biogenic compounds, are preserved in sedimentary rocks of low to moderate metamorphic grade over geologic time. These biomarkers, which are largely derived from membranes and photosynthetic pigments, and biosynthesised via highly conserved pathways, are modified *post mortem* according to known diagenetic processes and convey, with varying degrees of specificity, information about the identities and physiologies of their source organisms (Brassell et al., 1983; Ourisson et al., 1987; Brocks and Summons, 2003; Peters et al., 2004).

Biomarker studies of PTB sediments reveal a diversity of biogeochemical evidence for dramatic events. Sephton and others, for example, have measured trends in δ^{13}C of sedimentary carbonate and leaf wax-derived *n*-alkanes and abundances of oxygen-containing aromatic compounds in Permian sedimentary strata from northern Italy that suggest an end-Permian terrestrial ecosystem collapse and transport of this soil-derived organic matter to the ocean (Sephton et al., 2002; Sephton et al., 2005; Watson et al., 2005). Similar aromatic abundance data has been reported in an expanded section from Eastern Greenland (Fenton et al., 2007) where samples from the pre-collapse interval in this section were characterised by high abundances of dibenzofuran (DBF), dibenzothiophene (DBT) and biphenyl thought to be derived from phenolic compounds of lignin from defunct woody plants. Enhanced sedimentation of soil-derived organics was also recently reported in a study of outcrop samples from Beds 24–26 and 29–31 of the Meishan section where the distributions and isotopic compositions of hopanoid triterpanes (Wang, 2007) were invoked as evidence. Enrichment in the contents of dibenzofurans and lignin-derived alkyl phenols has also been reported for Meishan (Wang and Visscher, 2007). Bacterial biomarker anomalies at Meishan, specifically two episodes of enhancement in the abundances of 2-methylhopanoids, which potentially reflect cyanobacterial productivity (Summons et al., 1999), were reported by both Wang and Xie (Xie et al., 2005, 2007; Wang, 2007). These occurred in Beds 26 and 34 following the main documented extinction horizon at the base of Bed 25 at Meishan.

Prime examples of taxonomically and physiologically diagnostic biomarkers are the aromatic carotenoids produced abundantly by the green and purple sulfur bacteria. Isorenieratene and chlorobactene are two distinctive aromatic carotenoid pigments essential to light-harvesting by the brown and green strains of green sulfur bacteria (Chlorobiaceae) respectively. The Chlorobiaceae biosynthesise pigments with a 2,3,6-trimethyl aromatic substitution pattern and utilise the reversed TCA cycle for carbon assimilation leading to their biochemicals being enriched in ^{13}C compared to those produced by most other phototrophs (Summons and Powell, 1986; Hartgers et al., 1993; Grice et al., 1996, 1997). Further, these compounds are well preserved as the molecular fossils isorenieratane and chlorobactane, together with their derivative aryl isoprenoids (Koopmans et al., 1996; Sinninghe Damsté et al., 2001; Brocks and Summons, 2003).

Chlorobiaceae are strictly anaerobic, obligate phototrophs using mainly H_2S as an electron donor for photosynthesis; as plankton, they abound where euxinic conditions extend into the photic zone such as in the modern-day Black Sea (Overmann et al., 1992). Furthermore, the presence of environmental sulfide promotes their initial preservation as organo-sulfur compounds (OSC) which ultimately become reduced to the more stable hydrocarbons that have been used extensively as paleoenvironmental indicators of photic zone euxinia (PZE) (Summons and Powell, 1986; Summons and Powell, 1987; Hartgers et al., 1993; Grice et al., 1996; Koopmans et al., 1996; Pancost et al., 2002). Chlorobiaceae biomarkers have been shown to be present in PTB sediments from the Perth Basin, Meishan (Grice et al., 2005a) and in a section in the Peace River Basin (Hays et al., 2007).

In most PTB biomarker studies conducted to date, emphasis has been placed on events near to the main extinction horizon and its aftermath and this has been particularly enlightening in respect to documenting the 'soil crisis' and phytoplankton transitions (Sephton et al., 2005; Xie et al., 2005; Fenton et al., 2007; Wang and Visscher, 2007; Wang, 2007). However, few biomarker investigations have sought to unravel events occurring on longer timescales, especially in respect to examining paleoenvironmental conditions presaging the extinction. Accordingly, when samples became available as part of the Meishan Drilling Project, we undertook a detailed investigation of trends in biomarker and isotopic lipids through 214 m of section covering the late Wuchiapingian through Dienerian stages in the Lungtan, Changxing, Yinkeng and Helongshan formations.

2. The Meishan Drilling Project

The PTB succession exposed in quarries at Meishan, South China (Fig. 1), has been the focus of more than twenty years of detailed research into the paleontology and geochemistry of the mass extinction (Jin et al., 2000; Yin et al., 2001; Cao et al., 2002). Nevertheless, there remains a considerable amount of ambiguous and conflicting data that, in part, reflects the exposure of these rocks to intense surface weathering. In order to obtain a complete succession of rock samples unaffected by atmospheric exposure and free from outcrop contamination, a drilling project was instigated by the Nanjing Institute of Geology and Paleontology under the leadership of the late Professor Jin Yugan. Two cores, drilled at a site 550 m to the west of the Meishan Section D, afforded the best possible geochemical record of the environmental evolution at the GSSP, not only for the Permian–Triassic transition, but also for the entire Changhsingian Stage and post-extinction Induan

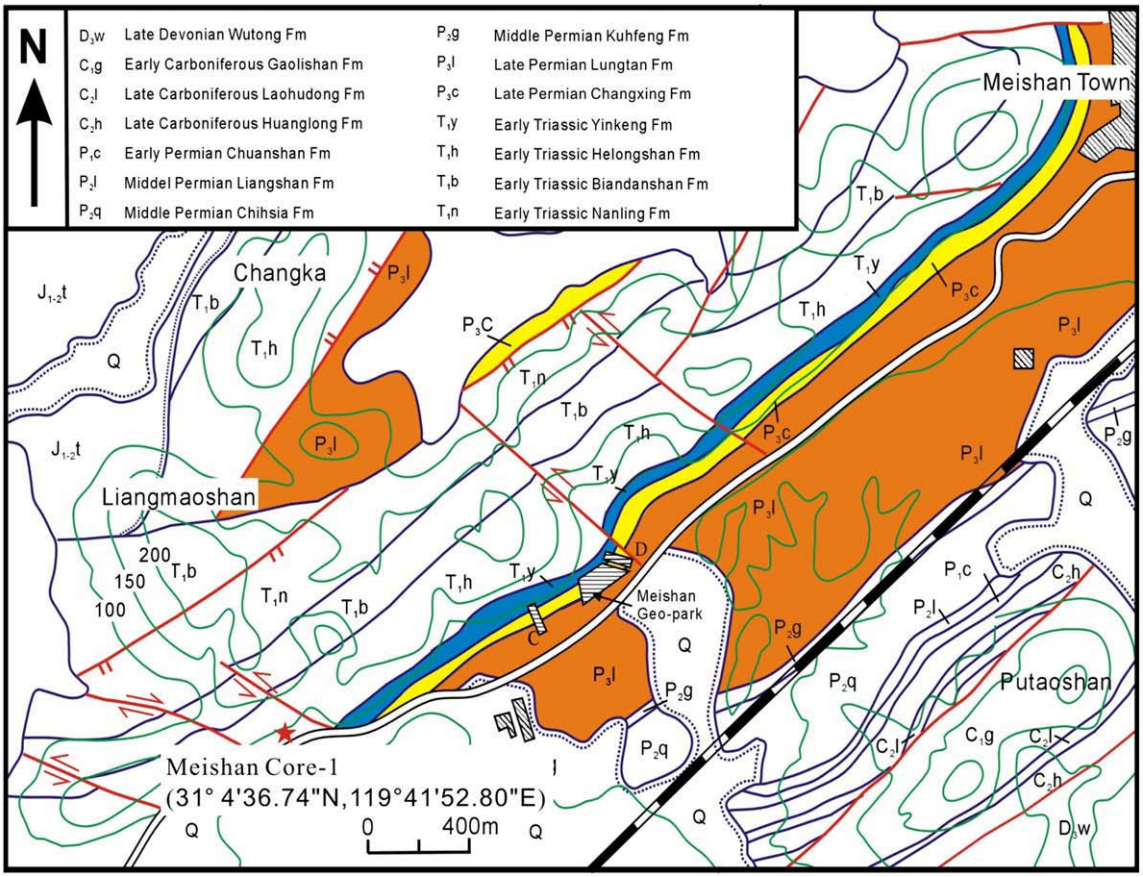

Fig. 1. A geological map of the Meishan locality and the site of the Meishan-1 core.

Stage of Early Triassic. Details of the samples and analytical methods are provided as supplementary online material.

3. Results and discussion

3.1. Isotopic data

Bulk geochemical parameters for the samples analysed in this study are plotted in the context of stratigraphic and lithologic relationships and relative sea-level (Fig. 2) (Zhang et al., 1996). The $\delta^{13}C_{carb}$ data (Fig. 2B) reported here are mostly those collected in the outcrop of Section D prior to drilling (Cao et al., 2002). A total of 371 samples span 158 m of section from the bottom of the Permian Changxing Fm. through the Triassic Helongshan Fm. Of these, 94 samples were from just 1.28 m of section across the Permian–Triassic boundary interval comprising Beds 24 to 27. This carefully conducted, high density sampling reveals that a minimum $\delta^{13}C_{carb}$ value of −3.23‰ is encountered only once at the topmost unit of Bed 24e just below the "boundary ash clay" of Bed 25 and not in Beds 26 and 27 and previously reported (Xu and Yan, 1993).

Some black sediment samples were collected for comparison of $\delta^{13}C_{carb}$ in selected horizons in the Changxing Fm. (Fig. 2B) and have more positive values. Considering the trends in $\delta^{13}C_{carb}$ in the Changhsingian stage from other sites, such as the Shangsi Section, where these more negative values are not encountered, this strongly suggests that these samples are diagenetically altered. Additional negative $\delta^{13}C_{carb}$ values measured in the basal part of Changxing Fm. are either in, or near, the calcite veins. They too likely contain diagenetically-altered carbonate.

The TOC and the organic carbon, nitrogen and strontium isotopic data shown in Fig. 2 are all from the Meishan-1 core. A number of clear and informative trends can be discerned. The very sharp negative excursion $\delta^{13}C_{carb}$ (Fig. 2B) culminates at the top of Bed 24 while the $\delta^{13}C_{org}$ values reach their minimum at the top of Bed 26 (Fig. 2C). Thus, the $\delta^{13}C_{org}$ minimum postdates the $\delta^{13}C_{carb}$ minimum and the signals do not co-vary as one would expect from a carbon cycle operating in steady state. If not due to factors reflecting C-cycle dynamics, the offset and large variability in $\delta^{13}C_{org}$ values might be a reflection of the mixing of some organic matter sources of different isotopic compositions. An overall drift to slightly more negative values in $\delta^{13}C_{carb}$ (ca. 1‰) and $\delta^{13}C_{org}$ (ca. 2‰) can be discerned over the entire sampled section. The $\delta^{13}C_{carb}$ data show two negative excursions corresponding to the maximum flooding surfaces through the intervals of Beds 34–35, Beds 21–22 and Beds 11–13 which are quite subtle. The major excursion extends from Bed 24 and continues through Bed 37, with the sharp spike at the top of Bed 24. In contrast to these progressive 'excursions' we observe much larger and apparently chaotic bed-to-bed variation in the $\delta^{13}C_{org}$ values. This is most readily explained by mixing of organic components of differing $\delta^{13}C_{org}$ compositions and possibly comprising end-member marine and weathered terrestrial components as described previously (Cao et al., 2002). A similar phenomenon can be seen in the organic carbon isotopic trends of the PTB sections of the Perth, Carnarvon and Bonaparte Basins of Western Australia (Gorter et al., 1995; Foster et al., 1997, 1998). A terrestrial component may include recently defunct plant-derived biomass from breakdown of terrestrial productivity (Sephton et al., 2005) but would most likely be dominated by weathered and re-worked fossil carbon including coal fragments (Faure et al., 1995; Foster et al., 1997).

Seawater $^{87}Sr/^{86}Sr$ values reflect a balance of radiogenic strontium inputs from both continental silicate weathering and the hydrothermal circulation at mid oceanic ridges (Palmer and Edmond, 1993). It is a useful proxy for tracking tectonic evolution (Veizer and Compston, 1976) and for Late Permian stratigraphic correlations worldwide (Faure et al., 1995; McArthur et al., 2001; Wang et al., 2007). The values of $^{87}Sr/^{86}Sr$ in Meishan carbonates (Fig. 2D) generally parallel

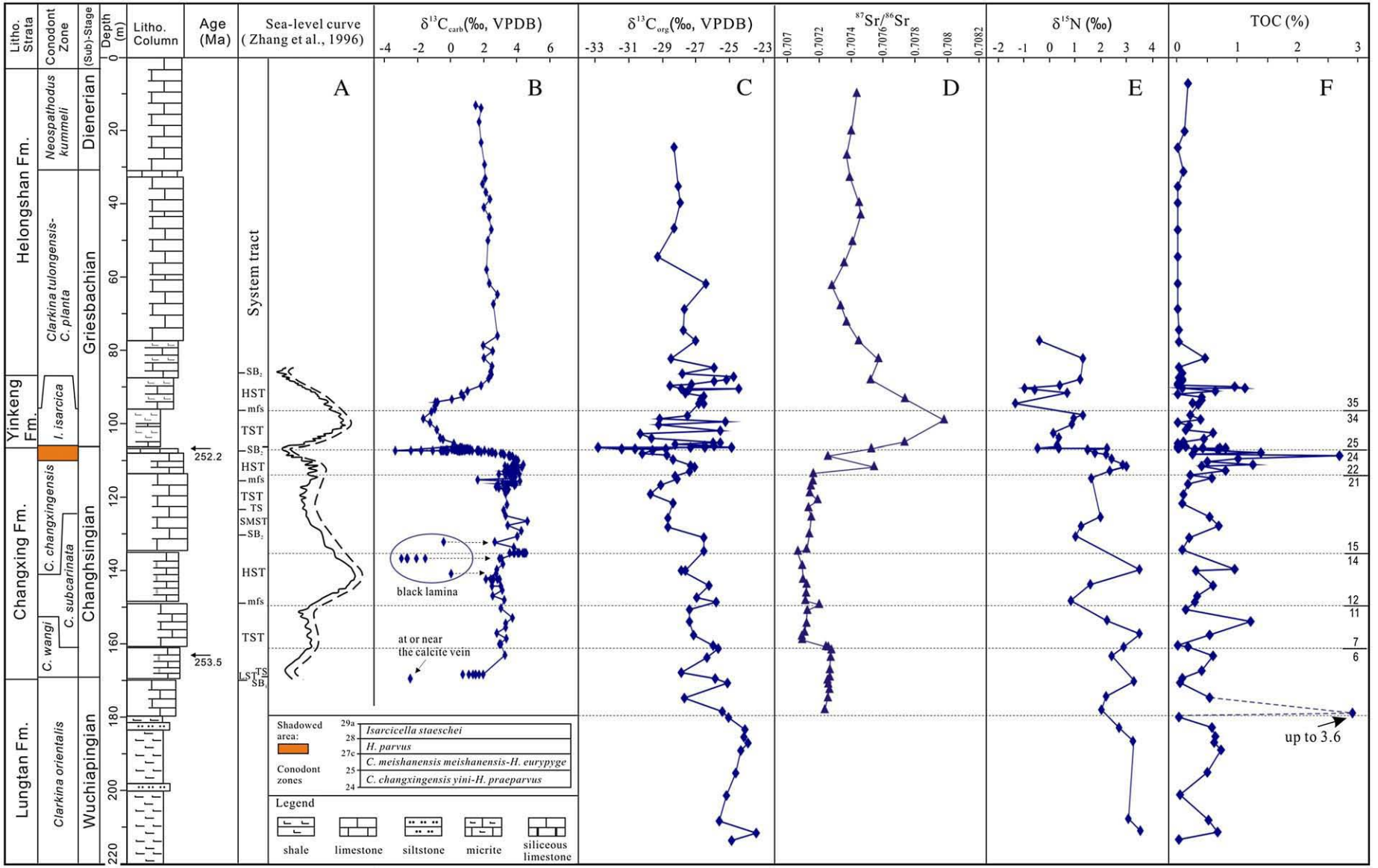

Fig. 2. Stratigraphy and lithology of the Meishan-1 core plotted together with a relative sea-level curve for the Changhsingian and basal Griesbachian stages. With the exception of $\delta^{13}C_{carb}$, which is a compilation of previously reported outcrop data and the Meishan core data (Cao et al., 2002), values of bulk geochemical parameters are for the samples measured in this study.

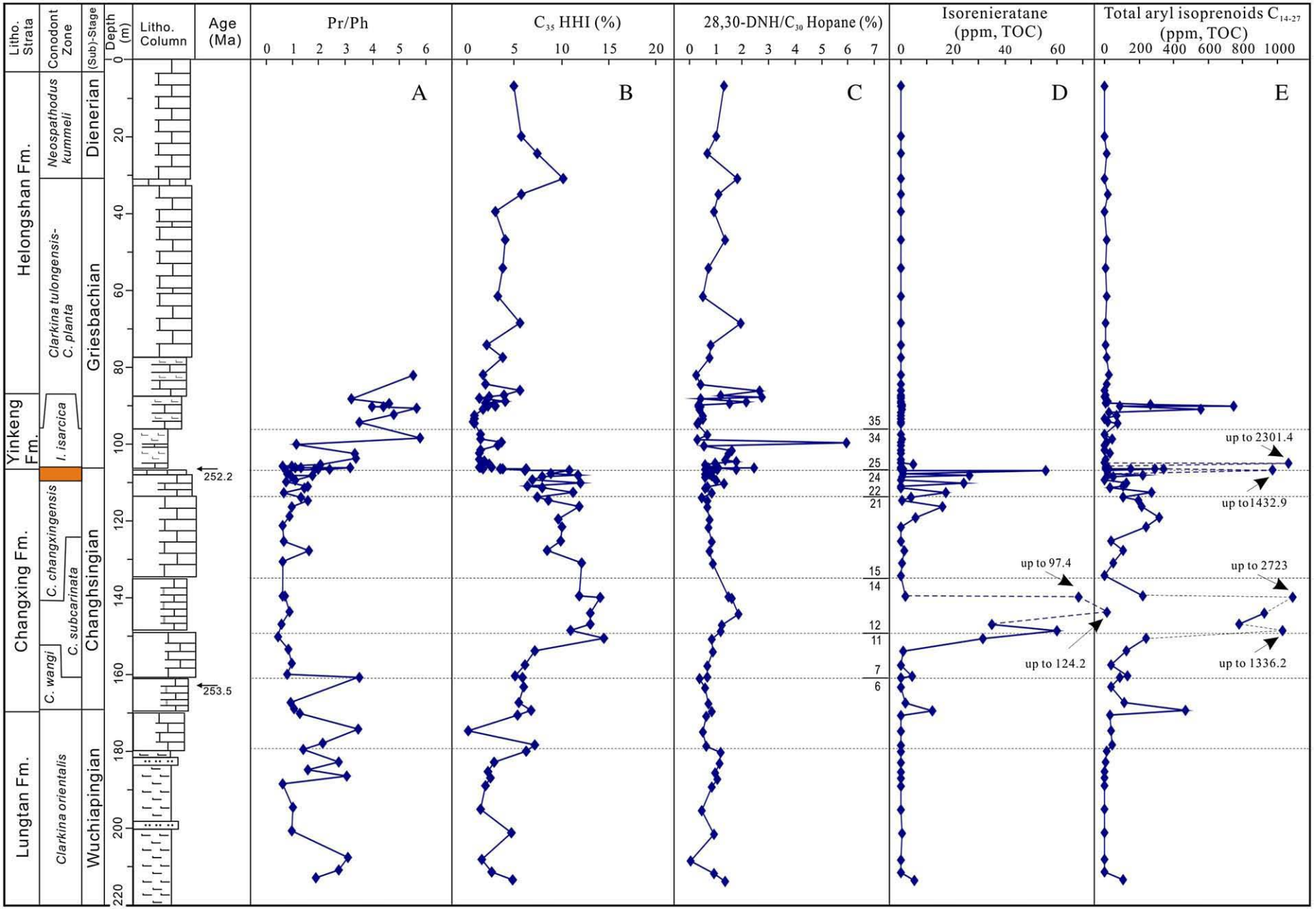

Fig. 3. Values of hydrocarbon-derived geochemical parameters diagnostic for water column and sedimentary redox conditions plotted against the Meishan-1 core stratigraphy. Pristane/phytane (Pr/Ph) data were calculated from the total ion currents of full scan GC-MS data. The C_{35}HHI (%), which is the abundance of C_{35} hopane 22S + 22R isomers as a percentage of the summed C_{31-35} homohopanes, and the abundance of 28,30-dinorhopane (28,30-DNH/ 28,30-DNH + C_{30} αβ-hopane *100) data were derived from GC-MS data run in MRM mode. The absolute abundances of isorenieratane and aryl isoprenoids, normalised to total organic carbon contents, were derived from GC-MS SIM data using an internal standard and calculated response factors.

the background seawater values suggested by McArthur et al. (2001) with values near 0.7072 for the Changhsingian stage and moving to more positive values around 0.7075 in lower Triassic strata. This accords with earlier findings (Faure et al., 1995; Korte et al., 2003, 2006). A small decrease in the claystone Beds 6–7 suggest volcanic input to the ocean while the progressive increase evident from Bed 15 onwards indicates a strong dominance of continental detritus during the latest Permian regression. Overall, the long-term trends in carbon and strontium isotopes are consistent with an extended period of enhanced weathering of both silicates and organic matter with the coincidence of strong opposing trends in $^{87}Sr/^{86}Sr$ and $\delta^{13}C_{carb}$ (Fig. 2B) starting at Bed 23 being particularly profound.

The trend in $\delta^{15}N$ of organic matter is also informative. Positive values of $\delta^{15}N_{org}$ (Fig. 2E) in the Lungtan Fm. reflect a normal and complex trophic structure and N-cycling through nitrate and are typical of values recorded for organic nitrogen formed in the modern ocean (Altabet and Francois, 1994). There is a progressive decrease through the Changhsingian stage and the positive values of the Permian then give way to zero and negative values at the top of Bed 24. Negative $\delta^{15}N_{org}$ persist into the Early Triassic Yinkeng Fm. although low contents of organic matter precluded $\delta^{15}N_{org}$ measurements above Bed 37. As with other Mesozoic Oceanic Anoxic Events (OAEs), a trend to zero and negative values of $\delta^{15}N_{org}$ is widely thought to reflect ecological disturbance and a nitrogen cycle with reduced involvement of oxidised species (nitrate and nitrite) and increased nitrogen fixation (Altabet and Francois, 1994). Based on strong correlations with increased abundances of hopanoid hydrocarbons, these 'light' nitrogen isotopic data are hypothesised to signal significantly enhanced cyanobacterial N-fixation (Kuypers et al., 2004; Dumitrescu and Brassell, 2006; Ohkouchi et al., 2006).

3.2. Redox-sensitive biomarkers

The patterns of biomarker trends in the Meishan-1 core indicate that biogeochemical changes that presaged the PTB extinction were both profound and prolonged. Trends in biomarker hydrocarbons (Fig. 3) that are considered diagnostic for water column redox conditions, such as the ratio of pristane to phytane (Pr/Ph), C_{35} homohopane index (C_{35}HHI) and relative abundance of 28,30-dinorhopane (28,30-DNH), are empirically linked to organic matter deposited in marine environments under strongly reducing conditions (Peters et al., 2004). However, these indices also reflect a complex interplay of diagenetic conditions, specific source inputs and sediment maturity that vary somewhat independently. As reported previously (Wang et al., 2005) a protracted interval with persistently low Pr/Ph (<1) values in the Changxing Fm. gives way to one with large fluctuations at and above Bed 25. The very low TOC and extract yield of samples from the Helongshan Formation precluded exact Pr/Ph measurements in this unit. However, in the Changxing Fm., the low Pr/Ph values are directly correlated with other parameters diagnostic of reducing and sulfidic conditions. The C_{35}HHI (Fig. 3B) records selective preservation of the intact C_{35} carbon skeleton of bacteriohopanepolyols under highly reducing conditions (Köster et al., 1997). The elevated (>5%) values of this parameter correlate well with low Pr/Ph ratios (Fig. 3A) and show that strongly reducing conditions persisted in the sediments from the top of the Lungtan Fm. and throughout the entire Changxing Fm. The relative abundance of 28,30-DNH as reflected by the value of the 28,30-DNH/C_{30}-hopane index shows somewhat higher values at maximum flooding (cf. Figs. 2A and 3C). Although the specific source of 28,30-DNH remains unknown, and the index is dependent on maturity and sediment lithology (Brincat and Abbott, 2001), its values in the range 0.5 to 2% suggests the entire cored section represents a reducing sedimentary environment (Seifert et al., 1978; Grantham et al., 1980; Schoell et al., 1992).

In contrast to the redox proxies based on acyclic isoprenoids (Pr/Ph) and bacteriohopanes (28, 30-DNH and C_{35}HHI), whose origins are multiple and complex, the aromatic carotenoid-derived biomarkers are very well established indicators for the physiological requirements (i.e. sunlight and H_2S) of the green sulphur bacteria (Summons and Powell, 1987; Brocks and Summons, 2003) and have previously been detected in the boundary section at Meishan (Grice et al., 2005a) and other oceanic anoxic events (Pancost et al., 2004; Ohkouchi et al., 2006; van Breugel et al., 2006). Isorenieratane and C_{14-27} aryl isoprenoids are present in the Meishan core samples through the entire section (Fig. 3D and E) from the Wuchiapingian Lungtan Fm., where they are in relatively low abundances, throughout the Changhsingian and Griesbachian stages. Notably, highest absolute abundances of isorenieratane (>5 ppm TOC) and the C_{14}–C_{27} aryl isoprenoids, and presumably the most persistent euxinic episodes, occur in zones encompassing Beds 11–15 – well in advance of the main extinction horizon and at Beds 24–25. Aryl isoprenoids then persist into the Triassic until the early Dienerian. The sediments encountered in the Meishan core alternate between shelf, slope and basinal environments and the *Chlorobium* biomarkers (Fig. 3D and E) are present at all stages of eustatic sea-level variation with maxima during the highstands (Fig. 2A). Modelling studies (Meyer et al., 2008) suggest that there would be spatial and secular variability in the intensity of shoaling of sulfidic waters into the photic zone and that this will be governed by bathymetry, nutrient fluxes and numerous other factors. Overall, PZE must have existed locally in the Eastern Tethys Ocean, at least intermittently, from c.254 Ma (Bowring et al., 1998) until ~251.4 Ma (Galfetti et al., 2007).

The biomarker data gathered from the Meishan sediments shows that the processes leading to euxinic conditions were protracted and persistent. This is consistent with sedimentological, paleontological and geochemical evidence for a widespread 'superanoxic' event (Isozaki, 1995; Wignall and Twitchett, 2002). Nevertheless, there are sections such as the carbonate reef sections at Ziyun and Laolongdong in South China and the Jiangyema section in Tibet that contain abundant benthic faunas not indicative of anoxic conditions in the Changhsingian and Wuchiapingian. Evidently, local topography and geography conferred variability in how anoxic/euxinic conditions affected shallow water environments.

3.3. Biomarkers indicative of the microbial community structure

Fig. 4 compares the distributions of a range of biomarkers that are often associated with specific taxonomic or physiological categories of microbes (Peters et al., 2004) The hopane/sterane ratio (H/S; Fig. 4A), a generalised proxy for the relative contributions of bacterial versus eukaryotic biomass shows exceedingly high values, throughout the entire section, compared to typical Phanerozoic values (0.5 to 2). In particular, the peaks in hopane/sterane in the Changxing (H/S = 31) and Yinkeng (H/S = 70) formations point to an ocean dominated by bacterial biomass and more resembling conditions recorded in Mesoproterozoic basins (Brocks et al., 2005). The proportions of steranes are also diagnostic for variability in the types of photosynthetic eukaryotes contributing organic matter to the sediments (Volkman, 1986; Volkman et al., 1998; Peters et al., 2004). In the marine realm, the proportion of C_{27} steranes (Fig. 4B) is generally higher than in non-marine environments and records variation in the balance of red over green algal communities. Low values can also be suggestive of significant inputs of vascular plant debris. This could be the case for samples from the Permian section where they are accompanied by elevated abundances of other plant-derived organic compound such as dibenzofurans (data not shown). A comparison of the C_{27}/C_{27-30} sterane ratio with the lithologies and sea-level curves of different orders suggests that an increase in the ratio, indicating a higher proportion of marine algal biomass, parallels the transitional phases of the 3rd-order sea-level (Haq et al., 1988; Zhang et al., 1996) in the Changhsingian stage. Here, the C_{27}/C_{27-30} sterane ratio shows similar trends to the relative abundance of gammacerane (Fig. 4C). Tetrahymanol, the precursor of gammacerane, is known to be produced by both purple non-sulfur bacteria and bacterivorous marine ciliates (Ten Haven et al., 1989; Kleemann et al., 1990;

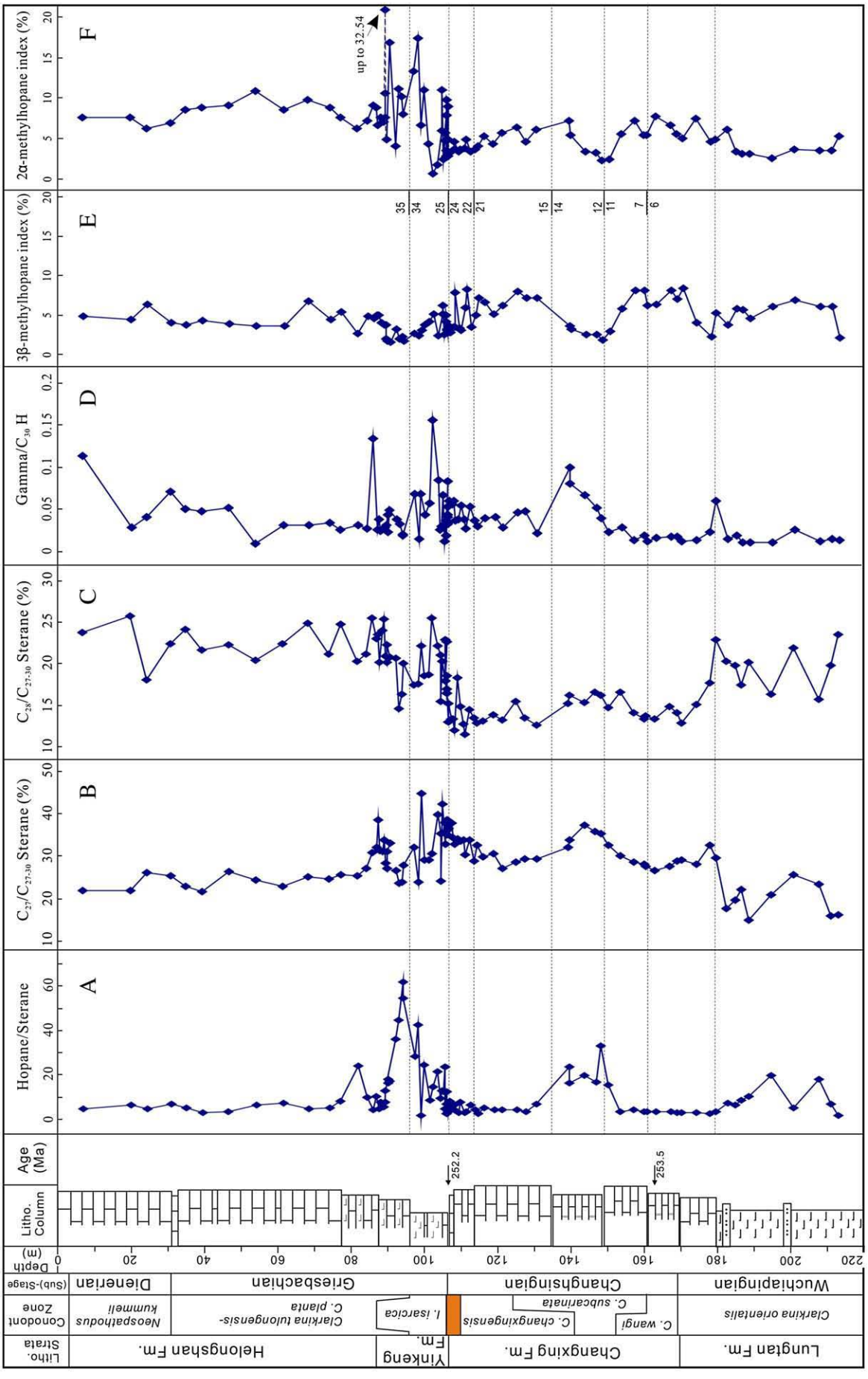

Fig. 4. Values of hydrocarbon-derived geochemical parameters diagnostic for components of the plankton communities plotted against the Meishan-1 core stratigraphy. All data were derived from GC-MS data collected in MRM mode using an internal standard for quantification. However, peak areas were not corrected for the different response factors of individual hydrocarbons. A: hopane/sterane ratio was calculated from the abundances of 19 isomers of the C_{27-35} hopanes and the main 24 isomers of the C_{27-30} steranes. B and C: The % C* sterane were calculated from C* Sterane abundance of diasteranes 20(R+S) and aaa plus abb (R + S) from C_{27} to C_{30}. D: Gamma/C_{30}H was the ratio of gammacerane to C_{30} αβ-hopane and E and F: 3β- and 2α-methylhopane indices were calculated from the percentage abundance of the C_{31} methylhopane relative to sum of C_{31} methylhopane and C_{30} αβ-hopane.

Harvey and McManus, 1991). Increased concentrations of its precursor, tetrahymanol, at the chemocline of stratified water columns appears to support a predominant origin from non-photosynthetic organisms, that is, ciliated protozoa that graze on algae and bacteria (Wakeham et al., 2007). In the late Permian H/S, C_{27}/C_{27-30} sterane and gammacerane/C_{30} hopane ratios peak together with the redox indicators C_{35}HHI, 28,30-DNH and aryl isoprenoids through Beds 10–14 of the Changxing Formation identifying this as a period where stratification and euxinia were most stable. In contrast, the values of most biomarker proxies fluctuate dramatically through the main extinction zone (Beds 22–26) and its immediate aftermath (Beds 27–35).

Increases in the proportion of C_{28} steranes (Fig. 4C) can record the relative importance of the chlorophyll C-containing plankton (dinoflagellates, diatoms and coccolithophorids); this is particularly evident in long timescale datasets when they rise to prominence during the Cenozoic (Knoll et al., 2007b). Here at Meishan, the proportion of C_{28} steranes is slightly elevated in Wuchiapingian, but significantly higher in the Griesbachian and Dienerian where values reach 25%, almost double the Changhsingian average. Although these sediments pre-date the middle Triassic dinoflagellate radiation, the traces of dinosteranes in these sediments record a presence of dinoflagellates around the PTB at Meishan. However, the abundances of dinosteranes are too low to discern any secular or paleoenvironmental trends. It is more likely that the overt increase in the C_{28} sterane signal through the Griesbachian records proliferation of prasinophytes in response to nitrate-N depletion and, possibly, other aspects of peturbed water column chemistry as observed elsewhere in the aftermath of OAEs (Prauss, 2007). Members of the Chlorodendrales, the most derived prasinophyte lineage, generally have a strong predominance of C_{28} sterols (Kodner et al., 2008).

It is also during this interval that carbonate deposition practically ceased and gave way to the clastic sedimentation recorded by the Yinkeng Fm. At the base of the Griesbachian stage, we observe the existence of conditions favourable for deposition of organic matter-rich and pyritic black shales during the basal Triassic transgressive phase (Fig. 2F). Very similar conditions are recorded in other basins at this time (Wignall and Twitchett, 2002) and, in the case of the Perth Basin, coincide with the development of thin intervals of petroleum-prone source rocks (Grice et al., 2005b). The co-eval and rapid fluctuations all the biomarker signals suggests an unstable and rapidly changing microbial community throughout the post-extinction flooding event (Fig. 2A).

Methylhopanes can be particularly useful for discerning specific bacterial physiologies (Talbot and Farrimond, 2007). As far as is known, 3β-methylbacteriohopanepolyols (3-MeBHP), precursors of 3β-methylhopanes, are derived from aerobic proteobacteria comprising methanotrophs and acetic acid bacteria (Rohmer et al., 1984; Zundel and Rohmer, 1985a,b). This is consistent with the prevalence of 3-MeBHP in environmental samples where methane-cycling is a significant biogeochemical process and observation of abundant 3β-methylhopanes in alkaline saline lakes (Collister et al., 1992; Talbot et al., 2003; Farrimond et al., 2004; Talbot and Farrimond, 2007). The abundances of both 2- and 3-methyl hopanes are generally measured relative to their non-methylated hopane equivalents using the 2-methylhopane index 2-MeHI (Summons et al., 1999) and analogous 3-MeHI. Values for the 3-MeHI at Meishan (Fig. 4E) are very high (1.6>3-MeHI<7) and elevated relative to values (1–3) typical of marine petroleum source rocks (Farrimond et al., 2004). Values of 3-MeHI (Fig. 4E) are highest in Beds 5–7 and Beds 15–18. However, there seems to be no direct relationship between high values for the 3-MeHI and the negative trends in $\delta^{13}C_{org}$ and $\delta^{13}C_{carb}$ suggesting that methane oxidation may be coupled to active methanogenesis associated with organic matter decay in a strongly oxygen- and sulfate-depleted environment, rather than being tied to any catastrophic release (Weidlich et al., 2003).

The 2-MeHI was originally proposed as a proxy for cyanobacterial input to sedimentary organic matter based on a combination of observations of the hopanoid contents for cultured organisms, natural environmental samples and the pattern of 2-methylhopane variations in the geological record (Summons et al., 1999; Kuypers et al., 2004; Knoll et al., 2007b; Sinninghe Damsté et al., 2008). Although alternative sources of 2-methylhopanoids are known, and specifically in a purple non-sulfur bacterium *Rhodopseudomonas palustris* (Rashby et al., 2007) and some other typically non-marine soil bacteria (Bisseret et al., 1985), these do not account for the patterns seen at Meishan or elsewhere in marine rocks and oils (Knoll et al., 2007b). Although tolerant of low concentrations of sulfide (Imhoff, 2006), *R. palustris* are not favoured by the euxinic conditions present at Meishan. Furthermore, *R. palustris* produces an abundance of methylated triterpenoids of the gammacerane type (Bravo et al., 2001; Rashby et al., 2007) which, so far, have not been reported in geological samples. Values of 2-MeHI (Fig. 4F) vary within a tight range from 5–7% for most of the late Permian section at Meishan. Dramatic fluctuations in the index are first seen at the PTB extinction horizon at Beds 24–25 as reported earlier (Xie et al., 2005) and continue during the Yinkeng Fm. In contrast to the earlier report, however, data from the Meishan-1 core show that the enhancement of the 2-MeHI occurs with numerous maxima with the highest being in Bed 37 (2-MeHI = 32.6).

The data for $\delta^{15}N_{org}$ (Fig. 2C) have their lowest values through Beds 24–37, the same interval as fluctuating 2-MeHI. This is consistent with the episodic loss of N-cycling through nitrate and, when this happens, a switch to N-fixing cyanobacterial primary producers (Dumitrescu and Brassell, 2006; Ohkouchi et al., 2006). At maximum flooding in the basal Triassic, we postulate a shoaling chemocline with greater utilization of newly fixed nitrogen and ^{15}N-depleted ammonium (Junium, 2007). The highest values in the H/S ratio (Fig. 4A) also occur here. Following the boundary event, in the interval of low $\delta^{15}N_{org}$, rapid fluctuations in redox (Pr/Ph) and repeated episodes of euxinia are evident as shown by the patterns of aryl isoprenoids (Fig. 3D and E). Therefore, we question whether there is a robust coupling between the 2-MeHI index and faunal extinction that was reported earlier (Xie et al., 2005). Rather, the fluctuating value for this parameter is likely yet another reflection of the instability of the Griesbachian microbial communities depicted in Figs. 2–5. Proliferation of various kinds of bacteria, including nitrogen-fixing cyanobacteria, and consequent elevation in the 2-MeHI index in the Griesbachian shales (Fig. 6C), was almost certainly a response to the paucity of nitrate in the water column following the extended euxinic conditions of the Late Permian.

3.4. Biomarker parameters influenced by maturity and lithology

The most enigmatic trends in the biomarkers of the Meishan-1 core occur in the ratios of compounds whose distributions depend on a combination of maturity, lithology and source (Figs. 5 and 6). The maturity of organic matter in samples from the Meishan-1 core is most reliably reflected in the ratio of the 22S/22S + 22R for C_{31} homohopanes (Fig. 5D). This parameter is an expression of isomerization at C-22 of the hopane side-chain and a stable end-point (~58–60%) is reached before the main phase of petroleum generation (Peters et al., 2004). The Meishan-1 values between 54 and 59% are highly consistent. Coupled to the range of the 20S/20S + 20R epimer ratio of the C_{27} steranes (45–50%), which measures a comparable isomerization, these suggest the entire sediment column is uniformly in the earliest stages of the 'oil window'.

The ratio of βα-hopanes (moretanes) to αβ-hopanes involves a more difficult isomerization in the hopane ring system and takes place at higher maturities than side-chain the side-chain epimerizations discussed above. When organic matter is immature for oil generation, with vitrinite reflectance values below 0.6–0.7, the ratio βα/αβ + βα of C_{30}-hopanes does not correlate with depth of burial and does not approach an end-point until the main phase of petroleum generation (Seifert and Moldowan, 1980; Grantham, 1986). Therefore, in the

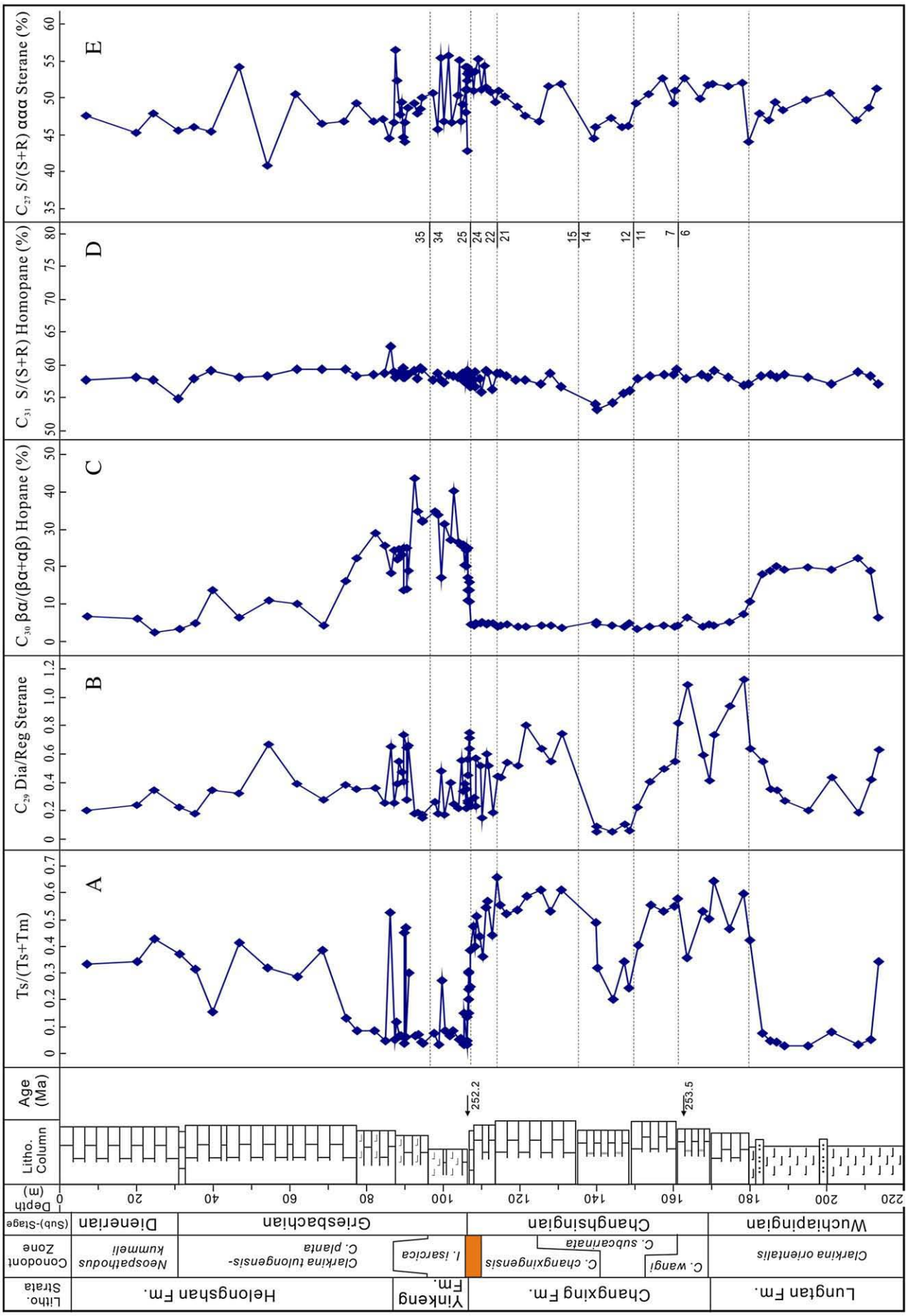

Fig. 5. Values of hydrocarbon-derived geochemical parameters diagnostic for thermal maturity and/or lithology plotted against the Meishan-1 core stratigraphy. All ratios were calculated from GC–MS data collected in the MRM mode. The individual ratios are as defined in the column headings.

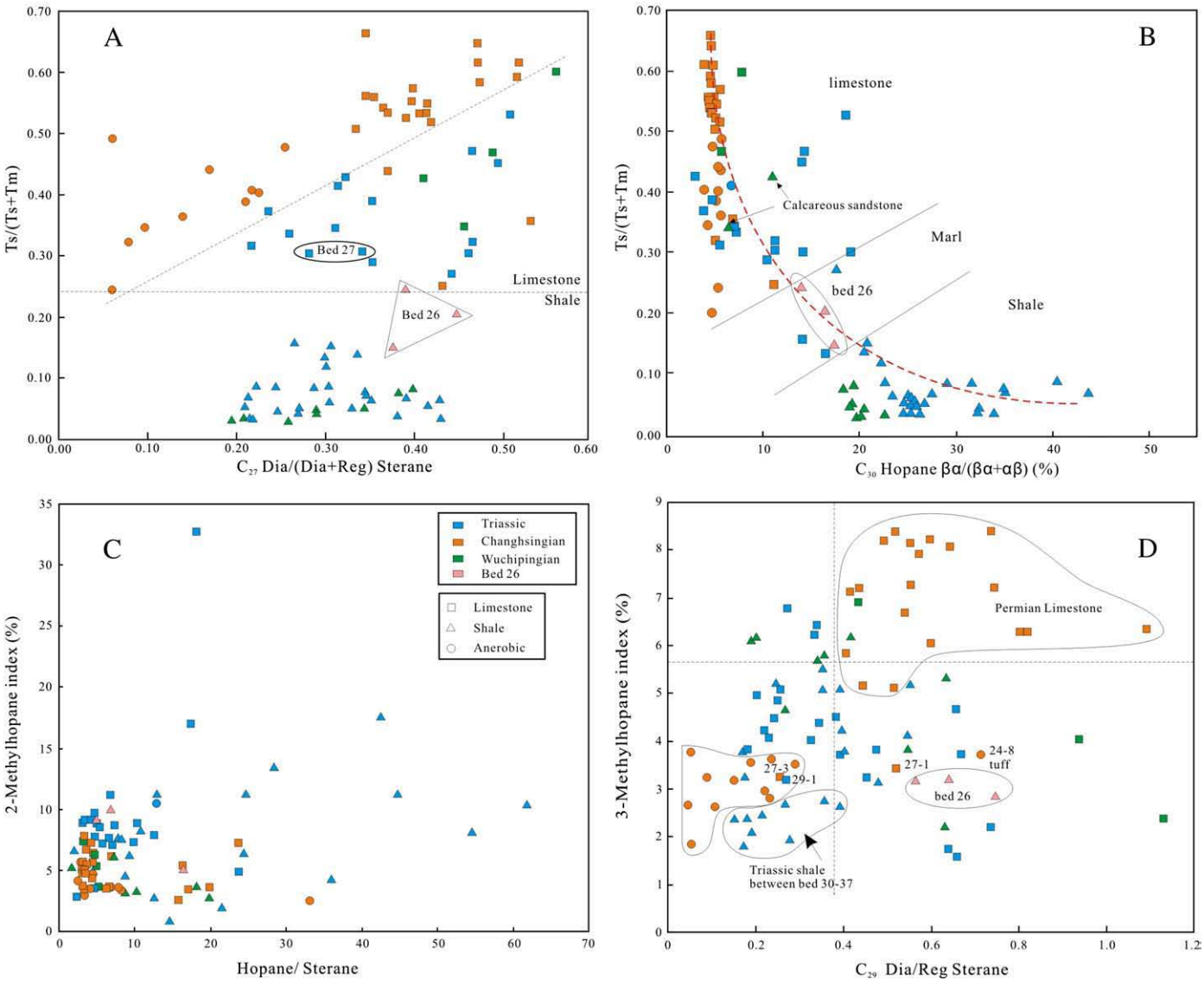

Fig. 6. Cross-correlations of various source and maturity parameters for the Meishan-1 core. Samples are color-coded according to age and lithology. The data display both strong and weak correlations indicative of the complex interplay between biomarker lipid sources and lithologies reflecting different styles of sedimentary diagenesis.

Meishan samples the ratio βα/αβ+ βα C_{30}-hopanes is a reflection of diagenetic conditions. Thus the step down in βα/αβ+βα C_{30}-hopanes near the top of the Lungtan Fm., and the step up again at the base of the Yinkeng Fm., are evidence of rapid transitions in paleoenvironment, organic matter source and diagenetic conditions.

During catagenesis, the abundance of the less stable C_{27} 17α-trisnorhopane (Tm or 17α-22,29,30-trisnorhopane) decreases relative to the more stable C_{27} 18α-trisnorneohopane (Ts) isomer as a function of burial depth (Seifert and Moldowan, 1978; Peters et al., 2004). However, the Ts/(Ts+Tm) ratio, like the relative abundance of moretanes, is also profoundly influenced by paleoenvironment and organic matter sources at low-moderate levels of thermal maturity (Moldowan et al., 1986). The Ts/(Ts+Tm) ratio is, therefore, most useful as a maturity indicator when samples are mature and of a common organofacies. The Ts/(Ts+Tm) ratio can also be a powerful indicator of changing environmental conditions and source biota, that is, organic matter inputs and sediment lithologies, as appears to be the case with the Meishan-1 core. Interestingly, the highest values of Ts/(Ts+Tm) are seen in the carbonate-dominated Permian section from the upper Lungtan Fm. and through most of the Changxing Fm. (Fig. 5A). Further, low values in the shale below 180 m in the Lungtan Fm. coincide with high values for βα/αβ+ βα C_{30}-hopanes (Fig. 5B), as would be expected if maturity was the dominant control. This phenomenon is further illustrated in the cross-plot of Fig. 6B. However, for a sediment column that has only experienced relatively shallow burial, and which shows no evidence of volcanic intrusion, the presence of an apparent 'mature' interval sandwiched between two 'less mature' ones is difficult to rationalise.

Anomalies in hopanoid maturity parameters for the Changxing and Yinkeng formations, and specifically the enhanced presence of βα-hopanes at Meishan have been noted previously (Wang, 2007; Xie et al., 2007) and attributed to input of terrestrial organic matter. However, these studies were conducted on outcrop samples and did not include detailed examination of the Lungtan Formation. Our data provide little support for this and, instead, suggest a more complex and long-lived scenario. Enhancement of βα-hopane abundances occurs in the Wuchiapingian and again at the PTB. High βα-hopane abundances occur more or less continuously starting from Bed 25 and show a more complex character with multiple maxima between Bed 26 and Bed 39. Some of the differences among studies might reflect

local variation in organic matter inputs and differences in preservation between core and outcrop samples. Regardless, the observed 'anomalous' behaviour of hopanoid maturity parameters, specifically the βα/βα + αβ-hopane and Ts/Ts + Tm ratios are best accounted for by secular change in diagenetic conditions. For example, Xie et al. (2007) suggested that the moretane anomaly could be a signal of increased terrestrial plant inputs resulting from enhanced continental weathering. This infers an origin of moretane from the array of C_{30} triterpenoids from ferns and, possibly, other primitive plants (Tsuzuki et al., 2001). However, the elevated moretane/hopane ratio is almost as high in the extended (C_{31+}) hopane series as it is in the C_{29} and C_{30} compounds (data not shown). In samples with very high βα/βα + αβ-hopane ratio, we observe a comparable elevation in the βα-isomers of the 2α-methylhopanes and the 3β-methylhopanes and their C_{32+} pseudohomologues. Thus, the 'moretane anomaly' is reflected in all three forms (desmethyl, 2-methyl and 3-methyl) of the extended hopanes and must, therefore, be a result of diagenetic conditions conducive to enhanced preservation of all βα-hopanoids.

4. Synthesis and conclusions

The biomarker and isotopic data gathered from Meishan-1 core point to a pattern of ecological disturbance and profound biogeochemical change that significantly predates the faunal transition marking the Permian Triassic boundary. Overt changes in biomarker distributions correspond to distinct lithological transitions toward the top of the Lungtan Fm. and, again, at the base of the Yinkeng Fm. Organic matter below 180 m in the core (Lungtan Fm.) is characterized by a predominance of C_{29} regular steranes, high hopane/sterane ratios and elevated relative abundances of βα-hopanes. Organic carbon and nitrogen isotopic values in this section record their highest values of −23.4 and +3.5‰ respectively. It appears feasible that, at this time of predominantly clastic sedimentation, the organic matter was of mostly marine origin together with some thermally mature terrestrial debris. Alternatively, the data are also consistent with predominantly authochthous inputs from a marine microbial community dominated by different kinds of bacteria.

A transition to carbonate deposition is recorded at ~10 m below the top of the Lungtan Formation at Meishan-1 core at 180 m and this continues throughout the Changxing Formation. These sediments were deposited under a continuously and intensely anoxic and euxinic water column as shown by the redox-sensitive proxies of low Pr/Ph ratios combined with elevated C_{35}HHI. Elevated sulfide concentrations existed in the photic zone as shown by the continuous presence of arylisoprenoids with highest concentrations recorded in Beds 11–14 of the Changhsingian stage. Importantly, the *Chlorobium* pigment derivatives are accompanied by a gradual and progressive drop in the $\delta^{15}N$ and $\delta^{13}C$ values of organic matter. A subtle negative excursion can be seen in the $\delta^{13}C_{carb}$ synchronously with the occurrence of elevated aryl isoprenoids and sea-level maximum through Beds 11–14.

The most profound biogeochemical changes become evident near to the main extinction horizon at Beds 24–25 where relative sea-level drops to a minimum and biomarkers provide evidence for intense euxinia. Strontium isotopes suggest a rapid intensification of weathering that is also marked by rapidly declining $\delta^{13}C$ values of carbonate carbon including the sharp spike at the point of maximum faunal change. It is here we also seen the first 'spike' in 2-MeHI, a minimum in $\delta^{15}N_{org}$ and many other changes in sterane and triterpane abundances. The following interval of shale deposition in the Yinkeng Formation is marked by rapid and dramatic fluctuations in most of the biomarker proxies measured. Evidently, the microbial community and composition of sedimentary organic matter were seeing extreme fluctuations with enhanced cyanobacterial primary productivity accompanied by profound anomalies triterpane stereoisomers. Peaks in the H/S ratio and the gammacerane/hopane ratio provide evidence for periods of heightened bacterial productivity and water-column stratification. Anomalous transitions in the βα/βα + αβ ratios of C_{29-30} hopanes, extended hopanes and methylhopanes point are not likely due to differences in thermal maturity, or a signal for collapse of the terrestrial ecosystem and allochthonous inputs of soil but, rather, a reflection of significant variability in the pathways of organic matter diagenesis. Some of these changes have been recognised previously and have been reported to occur as two distinct phases (Xie et al., 2005, 2007). However, our data, including the $\delta^{13}C_{carb}$ (Fig. 3B), $\delta^{13}C_{org}$ (Fig. 3C), 2-methylhopane index (Fig. 4F) and *Chlorobium* abundance (Fig. 3E) provide support for not just two, but for multiple episodes of enhanced bacterial productivity in the Early Triassic. Seen in the light of the extended record provided by the Meishan-1 core, the faunal turnover itself was presaged by long period of euxinic conditions beginning in the Wuchiapingian and continuing through the Changhsingian stage. Conditions unfavourable for O_2-respiring organisms did not appear suddenly but persisted for several millions of years prior to the extinction. Viewed alongside the pattern of taxon loss at Meishan (Jin et al., 2000) it can be seen that the gradual and continual loss in faunal diversity in the Changxing Fm., culminating in a sudden collapse in Beds 24–25, closely follows the pattern of biogeochemical change evident from the various biomarker and isotopic proxies. These factors must be taken into account when considering the agents responsible for such a pattern of biological change.

Numerous OAE's are in evidence in the geological record of the Phanerozoic. These are best documented in the Mesozoic Eon and often marked by negative C-isotopic excursions (Kump, 1991) although some are better known for the positive direction in $\delta^{13}C$ of inorganic carbon in high TOC shales as seen at the Toarcian and Frasnian–Famennian events (Hesselbo et al., 2000; Joachimski et al., 2001). One of the recurring themes that has attracted attention is the co-occurrence of high abundances of *Chlorobium* biomarkers, cyanobacterial 2-methylhopanoids and abnormally light values of $\delta^{15}N_{org}$ that have been interpreted as disruption of the N-cycle induced by euxinia. OAE's are further characterized by both transient (Kuypers et al., 2001) and long term (Falkowski et al., 2004; Falkowski and Knoll, 2007; Knoll et al., 2007b) changes in plankton communities pointing to the link between nitrogen budgets and plankton evolution and succession (Fennel et al., 2005). As the data shown in Figs. 2 and 4 suggest, cyanobacterial primary productivity was episodically enhanced after the faunal turnover, as evidenced by extreme fluctuations in the 2-methylhopane index and the zero to negative values in $\delta^{15}N_{org}$ data (Kuypers et al., 2004; Dumitrescu and Brassell, 2006). This could, therefore, be seen as a consequence of events leading up to the extinction and not necessarily a causal phenomenon. Instead, looking to events preceding the main phase of biological extinction, the evidence gathered in this study suggests the inception of euxinic conditions most likely has a geological underpinning in the final aggregation of Pangea with its associated volcanic, tectonic, climatic and continental weathering processes (Faure et al., 1995), combined with oceans predisposed to sluggish circulation patterns, instigating a super-anoxic episode lasting for millions of years (Isozaki, 1995, 2003).

Acknowledgements

The authors are grateful to numerous colleagues who provided encouragement, information and suggestions throughout this study. We are especially indebted to the late Professor Jin Yu-Gan who inspired our study of events at the Permian–Triassic boundary and who instigated the Meishan drilling project. Xiangdong Wang, Hua Zhang, Yue Wang and postgraduate students of the Late Paleozoic Research Group at Nanjing joined in the three-month drilling program and in collecting the cores. Kliti Grice, Emma Grosjean, Jürgen Rullkötter, Carolyn Colonero, Samuel Bowring, Douglas Erwin, Charles Henderson, Andrew Knoll and Tom Algeo provided invaluable suggestions and/or laboratory support.

NSF USA and NSF China enabled our participation in US-China Workshops in Geology and Paleontology that led to this collaboration. Research at Nanjing was supported by the 973 (2006CB806400) project of the MST of China, NSFC and the CAS/SAFEA International Partnership Program for Creative Research Teams. Research at MIT was supported by the NASA Exobiology Program (Grant# NNG05GN62G).

Appendix A. Supplementary data

Supplementary data associated with this article can be found, in the online version, at doi:10.1016/j.epsl.2009.02.012.

References

Algeo, T.J., Ellwood, B., Nguyen, T.K.T., Rowe, H., Maynard, J.B., 2007. The Permian–Triassic boundary at Nhi Tao, Vietnam: evidence for recurrent influx of sulfidic watermasses to a shallow-marine carbonate platform. Palaeogeogr. Palaeoclimat. Palaeoecol. 252 (1–2), 304–327.

Altabet, M.A., Francois, R., 1994. Sedimentary nitrogen isotopic ratio as a recorder for surface ocean nitrate utilization. Glob. Biogeochem. Cycles 8, 103–116.

Benton, M.J., 2003. When Life Nearly Died: The Greatest Mass Extinction of all Time. Thames and Hudson, London.

Berner, R., 2006. Carbon, sulfur and O2 across the Permian–Triassic boundary. J. Geochem. Explor. 88 (1–3), 416–418.

Bisseret, P., Zundel, M., Rohmer, M., 1985. Prokaryotic triterpenoids. 2. 2β-Methylhopanoids from *Methylobacterium organophilum* and *Nostoc muscorum*, a new series of prokaryotic triterpenoids. Eur. J. Biochem. 150, 29–34.

Bowring, S.A., Erwin, D.H., Jin, Y.G., Martin, M.W., Davidek, K., Wang, W., 1998. U/Pb zircon geochronology and tempo of the end-Permian mass extinction. Science 280 (5366), 1039–1045.

Bowring, S.A., Erwin, D.H., Isozaki, Y., 1999. The tempo of mass extinction and recovery: the end-Permian example. Proc. Natl. Acad. Sci. 96 (16), 8827–8828.

Brassell, S.C., Eglinton, G., Maxwell, J.R., 1983. The geochemistry of terpenoids and steroids. Biochem. Soc. Trans. 11, 575–586.

Bravo, J.M., Perzl, M., Hartner, T., Kannenberg, E.L., Rohmer, M., 2001. Novel methylated triterpenoids of the gammacerane series from the nitrogen-fixing bacterium *Bradyrhizobium japonicum* USDA 110. Eur. J. Biochem. 268 (5), 1323–1331.

Brincat, D., Abbott, G.D., 2001. Some aspects of the molecular biogeochemistry of laminated and massive rocks from the Naples Beach Section (Santa Barbara–Ventura Basin). In: Isaacs, C.M., Rullkotter, J. (Eds.), The Monterey Formation: From Rocks to Molecules (Ed. by C.M. Isaacs, J. Rullkotter). Columbia University Press, New York, pp. 140–149.

Brocks, J.J., Summons, R.E., 2003. Sedimentary hydrocarbons, biomarkers for early life. In: Heinrich, D.H.a.K.K.T. (Ed.), Treatise on Geochemistry (Ed. by D.H.a.K.K.T. Heinrich). Pergamon, Oxford, pp. 63–115.

Brocks, J.J., Love, G.D., Summons, R.E., Knoll, A.H., Logan, G.A., Bowden, S.A., 2005. Biomarker evidence for green and purple sulphur bacteria in a stratified Palaeoproterozoic sea. Nature 437 (7060), 866.

Campbell, I.H., Czamanske, G.K., Fedorenko, V.A., Hill, R.I., Stepanov, V., 1992. Synchronism of the Siberian Traps and the Permian–Triassic Boundary. Science 258 (5089), 1760–1763.

Cao, C., Wang, W., Jin, Y.G., 2002. Carbon isotope excursions across the Permian–Triassic boundary in the Meishan section, Zhejiang Province, China. Chin. Sci. Bull. 47, 1125–1129.

Collister, J.W., Summons, R.E., Lichtfouse, E., Hayes, J.M., 1992. An isotopic biogeochemical study of the Green River oil shale. Org. Geochem. 19 (1–3), 265.

Crowley, J.L., Bowring, S.A., Shen, S.Z., Wang, Y., Cao, C., Jin, Y.G., 2006. U–Pb zircon geochronology of the end-Permian mass extinction. Geochim. Cosmochim. Acta 70 (18, Supplement 1), A119.

Dumitrescu, M., Brassell, S.C., 2006. Compositional and isotopic characteristics of organic matter for the early Aptian Oceanic Anoxic Event at Shatsky Rise, ODP Leg 198. Palaeogeogr. Palaeoclimat. Palaeoecol. 235 (1–3), 168–191.

Erwin, D.H., 1994. The Permo-Triassic extinction. Nature 367, 231–236.

Erwin, D.H., 2006. Extinction: How Life on Earth Nearly Ended 250 Million Years Ago. Princeton University Press, Princeton.

Falkowski, P., Knoll, A.H., 2007. In: Falkwoski, P., Knoll, A.H. (Eds.), The Evolution of Photosynthetic Organisms in the Oceans. In: The Evolution of Photosynthetic Organisms in the Oceans. Elsevier, Boston, pp. 133–163.

Falkowski, P.G., Katz, M.E., Knoll, A.H., Quigg, A., Raven, J.A., Schofield, O., Taylor, F.J.R., 2004. The evolution of modern eukaryotic phytoplankton. Science 305 (5682), 354–360.

Farrimond, P., Talbot, H.M., Watson, D.F., Schulz, L.K., Wilhelms, A., 2004. Methylhopanoids: Molecular indicators of ancient bacteria and a petroleum correlation tool. Geochim. Cosmochim. Acta 68 (19), 3873–3882.

Faure, K., de Wit, M.J., Willis, J.P., 1995. Late Permian global coal hiatus linked to 13C-depleted CO2 flux into the atmosphere during the final consolidation of Pangea. Geology 23 (6), 507–510.

Fennel, K., Follows, M., Falkowski, P.G., 2005. The co-evolution of the nitrogen, carbon and oxygen cycles in the Proterozoic ocean. Am. J. Sci. 305 (6–8), 526–545.

Fenton, S., Grice, K., Twitchett, R.J., Böttcher, M.E., Looy, C.V., Nabbefeld, B., 2007. Changes in biomarker abundances and sulfur isotopes of pyrite across the Permian–Triassic (P/Tr) Schuchert Dal section (East Greenland). Earth Planet. Sci. Lett. 262 (1–2), 230–239.

Foster, C., Logan, G., Summons, R.E., Gorter, J., Edwards, D., 1997. Carbon isotopes, kerogen types and the Permian–Triassic boundary in Australia: implications for exploration. Aust. Petrol. Prod. Explor. Assoc. J. 37, 442–459.

Foster, C.B., Logan, G.A., Summons, R.E., 1998. The Permian–Triassic boundary in Australia: where is it and how is it expressed? Proc. R. Soc. Vic. 110, 247–266.

Galfetti, T., Bucher, H., Ovtcharova, M., Schaltegger, U., Brayard, A., Brühwiler, T., Goudemand, N., Weissert, H., Hochuli, P.A., Cordey, F., Guodun, K., 2007. Timing of the Early Triassic carbon cycle perturbations inferred from new U–Pb ages and ammonoid biochronozones. Earth Planet. Sci. Lett. 258 (3–4), 593–604.

Gorter, J., Foster, C.B., Summons, R.E., 1995. Carbon isotopes and the Permian–Triassic boundary in the north Perth, Bonaparte and Carnarvon Basins, Western Australia. Petrol. Explor. Soc. Aust. J. 24, 21–38.

Grantham, P.J., 1986. Sterane isomerisation and moretane/hopane ratios in crude oils derived from Tertiary source rocks. Org. Geochem. 9 (6), 293–304.

Grantham, P.J., Posthuma, J., DeGroot, K., 1980. Variation and significance of the C27 and C28 triterpane content of a North Sea core and various North Sea crude oils. In: Douglas, A.G., Maxwell, J.R. (Eds.), Advances in Organic Geochemistry 1979 (Ed. by A.G. Douglas, J.R. Maxwell). Pergamon Press, New York, pp. 29–38.

Grice, K., Schaeffer, P., Schwark, L., Maxwell, J.R., 1996. Molecular indicators of palaeoenvironmental conditions in an immature Permian shale (Kupferschiefer, Lower Rhine Basin, north-west Germany) from free and S-bound lipids. Org. Geochem. 25 (3–4), 131–147.

Grice, K., Schaeffer, P., Schwark, L., Maxwell, J.R., 1997. Changes in palaeoenvrionmental conditions during deposition of the Permian Kupferschiefer (Lower Rhine Basin, northwest Germany) inferred from molecular and isotopic compositions of biomarker components. Org. Geochem. 26 (11–12), 677–690.

Grice, K., Cao, C., Love, G.D., Bottcher, M.E., Twitchett, R.J., Grosjean, E., Summons, R.E., Turgeon, S.C., Dunning, W., Jin, Y., 2005a. Photic zone euxinia during the Permian–Triassic superanoxic event. Science 307 (5710), 706–709.

Grice, K., Summons, R.E., Grosjean, E., Twichett, R.J., Dunning, W., Wang, S.X., Boettcher, M.E., 2005b. Novel depositional conditions of the Northern Onshore Perth Basin (Basal Triassic). AAPEA J. 45, 263–273.

Haq, B.U., Hardenbol, J., Vail, P.R., 1988. Mesozoic and Cenozoic chronostratigraphy and cycles of sea-level change. In: Wilgus, C.K., Hastings, B.S., Posamentier, H., Wagoner, J.V., Ross, C.A., Kendall, C.g.S.C. (Eds.), Sea-Level Changes – An Integrated Approach SEPM Special Publication 42 (Ed. by C.K. Wilgus, B.S. Hastings, H. Posamentier, J.V. Wagoner, C.A. Ross, C.g.S.C. Kendall), pp. 71–108.

Hartgers, W.A., Sinninghe Damsté, J.S., Requejo, A.G., Allan, J., Hayes, J.M., Ling, Y., Tiang-Min, X., Primack, J., de Leeuw, J.W., 1993. A molecular and carbon isotopic study towards the origin and diagenetic fate of diaromatic carotenoids. Org. Geochem. 22, 703–725.

Harvey, H.R., McManus, G.B., 1991. Marine ciliates as a widespread source of tetrahymanol and hopan-3B-ol in sediments. Geochim. Cosmochim. Acta 55, 3387–3390.

Hays, L., Beatty, T., Henderson, C.M., Love, G.D., Summons, R.E., 2007. Evidence for photic zone euxinia through the end-Permian mass extinction in the Panthalassic Ocean (Peace River Basin, Western Canada). Palaeoworld 16 (1–3), 39–50.

Hesselbo, S.P., Grocke, D.R., Jenkyns, H.C., Bjerrum, C.J., Farrimond, P., Morgans Bell, H.S., Green, O.R., 2000. Massive dissociation of gas hydrate during a Jurassic oceanic anoxic event. Nature 406 (6794), 392.

Holser, W.T., 1977. Catastrophic chemical events in the history of the ocean. Nature 267 (5610), 403.

Holser, W.T., Schonlaub, H.-P., Attrep, M., Boeckelmann, K., Klein, P., Magaritz, M., Orth, C.J., Fenninger, A., Jenny, C., Kralik, M., Mauritsch, H., Pak, E., Schramm, J.-M., Stattegger, K., Schmoller, R., 1989. A unique geochemical record at the Permian/Triassic boundary. Nature 337 (6202), 39.

Imhoff, J., 2006. The phototrophic Alpha-proteobacteria. In: Dworkin, M., Falkow, S., Rosenberg, E., Schleifer, K.-H., Stackebrandt, E. (Eds.), The Prokaryotes: A Handbook on the Biology of Bacteria, 5 (Ed. by M. Dworkin, S. Falkow, E. Rosenberg, K.-H. Schleifer, E. Stackebrandt). Springer, pp. 41–64.

Isozaki, Y., 1995. Superanoxia across the Permo-Triassic boundary: record in accreted deep-sea pelagic chert in Japan. Mem. – Can. Soc. Pet. Geol. 17, 805–812.

Isozaki, Y., 1997. Permo-Triassic boundary superanoxia and stratified superocean: records from lost Deep Sea. Science 276 (5310), 235–238.

Isozaki, Y., 2003. Guadalupian–Lopingian boundary event in mid-Panthalassa: correlation of accreted deep-sea chert and mid-oceanic atoll carbonate. In: Wong, T.E. (Ed.), XVth International Congress on Carboniferous and Permian Stratigraphy. Royal Netherlands Academy of Arts and Sciences, Utrecht, pp. 111–124.

Jin, Y., Wang, Y., Wang, W., Shang, Q.H., Cao, C., Erwin, D.H., 2000. Pattern of marine mass extinction near the Permian–Triassic boundary in South China. Science 289, 432–436.

Jin, Y., Wang, Y., Henderson, C.M., Wardlaw, B.R., Shen, S., Cao, C., Wang, W., 2006. The Global Stratotype Section and Point (GSSP) for the base-Changhsingian Stage (Upper Permian). Episodes 29 (3), 175–182.

Joachimski, M.M., Ostertag-Henning, C., Pancost, R.D., Strauss, H., Freeman, K.H., Littke, R., Sinninghe Damste, J.S., Racki, G., 2001. Water column anoxia, enhanced productivity and concomitant changes in [delta]13C and [delta]34S across the Frasnian–Famennian boundary (Kowala – Holy Cross Mountains/Poland). Chem. Geol. 175 (1–2), 109.

Junium, C.K.A., M.A., 2007. Nitrogen cycling during the Cretaceous, Cenomanian–Turonian Oceanic Anoxic Event II. Geochem. Geophys. Geosyst. 8 (3) ID Q03002.

Kamo, S.L., Czamanske, G.K., Krogh, T.E., 1996. A minimum U–Pb age for Siberian flood-basalt volcanism. Geochim. Cosmochim. Acta 60 (18), 3505.

Kamo, S.L., Czamanske, G.K., Amelin, Y., Fedorenko, V.A., Davis, D.W., Trofimov, V.R., 2003. Rapid eruption of Siberian flood-volcanic rocks and evidence for coincidence

with the Permian–Triassic boundary and mass extinction at 251 Ma. Earth Planet. Sci. Lett. 214 (1–2), 75–91.
Kleemann, G., Poralla, K., Englert, G., Kjøsen, H., Liaaen-Jensen, S., Neunlist, S., Rohmer, M., 1990. Tetrahymanol from the phototrophic bacterium *Rhodopseudomonas palustris*: first report of a gammacerane triterpene from a prokaryote. J. Gen. Microbiol. 136, 2551–2553.
Knoll, A.H., Bambach, R.K., Canfield, D.E., Grotzinger, J.P., 1996. Comparative Earth History and Late Permian Mass Extinction. Science 273, 452–457.
Knoll, A.H., Bambach, R.K., Payne, J.L., Pruss, S., Fischer, W.W., 2007a. Paleophysiology and end-Permian mass extinction. Earth Planet. Sci. Lett. 256 (3–4), 295.
Knoll, A.H., Summons, R.E., Waldbauer, J.R., Zumberge, J., 2007b. The geological succession of primary producers in the oceans. In: Falkwoski, P., Knoll, A.H. (Eds.), The Evolution of Photosynthetic Organisms in the Oceans (Ed. by P. Falkwoski, A.H. Knoll). Elsevier, Boston, pp. 133–163.
Kodner, R.B., Pearson, A., Summons, R.E., Knoll, A.H., 2008. Sterols in red and green algae: quantification, phylogeny, and relevance for the interpretation of geologic steranes. Geobiology 6 (4), 411–420.
Koopmans, M.P., Köster, J., Van Kaam-Peters, H.M.E., Kenig, F., Schouten, S., Hartgers, W.A., de Leeuw, J.W., Sinninghe Damste, J.S., 1996. Diagenetic and catagenetic products of isorenieratene: molecular indicators for photic zone anoxia. Geochim. Cosmochim. Acta 60 (22), 4467.
Korte, C., Kozur, H.W., Bruckschen, P., Veizer, J., 2003. Strontium isotope evolution of Late Permian and Triassic seawater. Geochim. Cosmochim. Acta 67 (1), 47–62.
Korte, C., Kozur, H.W., Joachimski, M.M., Strauss, H., Veizer, J., Schwark, L., 2004. Carbon, sulfur, oxygen and strontium isotope records, organic geochemistry and biostratigraphy across the Permian/Triassic boundary in Abadeh, Iran. Int. J. Earth Sci. 93 (4), 565.
Korte, C., Jasper, T., Kozur, H.W., Veizer, J., 2006. $^{87}Sr/^{86}Sr$ record of Permian seawater. Palaeogeogr. Palaeoclimat. Palaeoecol. 240 (1–2), 89–107.
Köster, J., Van Kaam-Peters, H.M.E., Koopmans, M.P., De Leeuw, J.W., Sinninghe Damste, J.S., 1997. Sulphurisation of homohopanoids: effects on carbon number distribution, speciation, and 22S/22R epimer ratios. Geochim. Cosmochim. Acta 61 (12), 2431–2452.
Kump, L., 1991. Interpreting carbon-isotope excursions: strangeloveoceans. Geology 19, 299–302.
Kump, L.R., Pavlov, A., Arthur, M.A., 2005. Massive release of hydrogen sulfide to the surface ocean and atmosphere during intervals of oceanic anoxia. Geology 33, 397–400.
Kuypers, M.M.M., Blokker, P., Erbacher, J., Kinkel, H., Pancost, R.D., Schouten, S., Sinninghe Damste, J.S., 2001. Massive expansion of marine Archaea during a Mid-Cretaceous oceanic anoxic event. Science 293 (5527), 92–95.
Kuypers, M.M.M., van Breugel, Y., Schouten, S., Erba, E., Damste, J.S.S., 2004. N2-fixing cyanobacteria supplied nutrient N for Cretaceous oceanic anoxic events. Geology 32 (10), 853–856.
McArthur, J.M., Howarth, R.J., Bailey, T.R., 2001. Strontium isotope stratigraphy: LOWESS Version 3: Best fit to the marine Sr-isotope curve for 0–509 Ma and accompanying look-up table for deriving numerical age. J. Geol. 109 (2), 155–170.
Meyer, K.M., Kump, L.R., Ridgwell, A., 2008. Biogeochemical controls on photic-zone euxinia during the end-Permian mass extinction. Geology 36 (9), 747–750.
Moldowan, J.M., Sundararaman, P., Schoell, M., 1986. Sensitivity of biomarker properties to depositional environment and/or source input in the lower Toarcian of SW-Germany. In: Leythaeuser, D., Rullkötter, J. (Eds.), Advances in Organic Geochemistry 1985, Org. Geochem., 10 (Ed. by D. Leythaeuser, J. Rullkötter). Pergamon, pp. 915–926.
Mundil, R., Ludwig, K.R., Metcalfe, I., Renne, P.R., 2004. Age and timing of the Permian mass extinctions: U/Pb dating of closed-system zircons. Science 305 (5691), 1760–1763.
Newton, R.J., Pevitt, E.L., Wignall, P.B., Bottrell, S.H., 2004. Large shifts in the isotopic composition of seawater sulphate across the Permo-Triassic boundary in northern Italy. Earth Planet. Sci. Lett. 218 (3–4), 331–345.
Ohkouchi, N., Kashiyama, Y., Kuroda, J., Ogawa, N.O., Kitazato, H., 2006. An importance of diazotrophic cyanobacteria as a primary producer during Cretaceous Oceanic Anoxic Event 2. Biogeosci. Discuss. 3, 575–605.
Ourisson, G., Rohmer, M., Poralla, K., 1987. Prokaryotic hopanoids and other polyterpenoid sterol surrogates. Annu. Rev. Microbiol. 41, 301–333.
Overmann, J., Cypionka, H., Pfenning, N., 1992. An extremely low-light-adapted phototrophic sulfur bacterium from the Black Sea. Limnol. Oceanogr. 37 (1), 150–155.
Palmer, M.R., Edmond, J.M., 1993. Uranium in river water. Geochim. Cosmochim. Acta 57 (20), 4947–4955.
Pancost, R.D., Crawford, N., Magness, S., Turner, A., Jenkyns, H.C., Maxwell, J.R., 2004. Further evidence for the development of photic-zone euxinic conditions during Mesozoic oceanic anoxic events. J. Geol. Soc. 161 (3), 353–364.
Pancost, R.D., Crawford, N., Maxwell, J.R., 2002. Molecular evidence for basin-scale photic zone euxinia in the Permian Zechstein Sea. Chem. Geol. 188, 217–227.
Payne, J.L., Kump, L.R., 2007. Evidence for recurrent Early Triassic massive volcanism from quantitative interpretation of carbon isotope fluctuations. Earth Planet. Sci. Lett. 256 (1–2), 264–306.
Payne, J.L., Lehrmann, D.J., Wei, J., Orchard, M.J., Schrag, D.P., Knoll, A.H., 2004. Large perturbations of the carbon cycle during recovery from the end-Permian extinction. Science 305 (5683), 506–509.
Peters, K.E., Moldowan, J.M., Walters, C.C., 2004. The Biomarker Guide. Cambridge University Press, Cambridge, UK.
Prauss, M.L., 2007. Availability of reduced nitrogen chemospecies in photic-zone waters as the ultimate cause of fossil prasinophyte prosperity. Palaios 22 (5), 489–499.
Rashby, S.E., Sessions, A.L., Summons, R.E., Newman, D.K., 2007. Biosynthesis of 2-methylbacteriohopanepolyols by an anoxygenic phototroph. Proc. Natl. Acad. Sci. U. S. A. 104 (38), 15099–15104.
Raup, D.M., Sepkoski, J.J.J., 1982. Mass extinctions in the marine fossil record. Science 215 (4539), 1501–1503.
Riccardi, A.L., Arthur, M.A., Kump, L.R., 2006. Sulfur isotopic evidence for chemocline upward excursions during the end-Permian mass extinction. Geochim. Cosmochim. Acta (70), 5740–5752.
Rohmer, M., Bouvier-Nave, P., Ourisson, G., 1984. Distribution of hopanoid triterpenes in prokaryotes. J. Gen. Microbiol. 130, 1137–1150.
Schoell, M., McCaffrey, M.A., Fago, F.J., Moldowan, J.M., 1992. Carbon isotopic compositions of 28,30-bisnorhopanes and other biological markers in a Monterey crude oil. Geochim. Cosmochim. Acta 56 (3), 1391–1399.
Seifert, W.K., Moldowan, J.M., 1978. Applications of steranes, terpanes and monoaromatics to the maturation, migration and source of crude oils. Geochim. Cosmochim. Acta 42, 77–95.
Seifert, W.K., Moldowan, J.M., 1980. The effect of thermal stress on source rock quality as measured by hopane stereochemistry. In: Douglas, A.G., Maxwell, J.R. (Eds.), Advances in Organic Geochemistry 1979 (Ed. by A.G. Douglas, J.R. Maxwell). Pergamon Press, Oxford, pp. 229–237.
Seifert, W.K., Moldowan, J.M., Smith, G.W., Whitehead, E.V., 1978. First proof of structure of a C28-pentacyclic triterpane in petroleum. Nature 271, 436–437.
Sephton, M.A., Looy, C.V., Veefkind, R.J., Brinkhuis, H., De Leeuw, J.W., Visscher, H., 2002. Synchronous record of d13C shifts in the oceans and atmosphere at the end of the Permian. Spec. Pap. – Geol. Soc. Am. 356, 455–462.
Sephton, M.A., Looy, C.V., Brinkhuis, H., Wignall, P.B., de Leeuw, J.W., Visscher, H., 2005. Catastrophic soil erosion during the end-Permian biotic crisis. Geology 33 (12), 941–944.
Sinninghe Damsté, J.S., Schouten, S., van Duin, A.C.T., 2001. Isorenieratene derivatives in sediments: possible controls on their distribution. Geochim. Cosmochim. Acta 65, 1557–1571.
Sinninghe Damsté, J.S., Kuypers, M.M.M., Pancost, R.D., Schouten, S., 2008. The carbon isotopic response of algae, (cyano)bacteria, archaea and higher plants to the late Cenomanian perturbation of the global carbon cycle: Insights from biomarkers in black shales from the Cape Verde Basin (DSDP Site 367). Org. Geochem. 39 (12), 1703–1718.
Summons, R.E., Powell, T.G., 1986. Chlorobiaceae in Paleozoic seas revealed by biological markers, isotopes and geology. Nature 319, 763–765.
Summons, R.E., Powell, T.G., 1987. Identification of aryl isoprenoids in source rocks and crude oils: biological markers for the green sulphur bacteria. Geochim. Cosmochim. Acta 51, 557–566.
Summons, R.E., Jahnke, L.L., Hope, J.M., Logan, G.A., 1999. 2-Methylhopanoids as biomarkers for cyanobacterial oxygenic photosynthesis. Nature 400, 554–557.
Talbot, H.M., Farrimond, P., 2007. Bacterial populations recorded in diverse sedimentary biohopanoid distributions. Org. Geochem. 38 (8), 1212–1225.
Talbot, H.M., Watson, D.F., Pearson, E.J., Farrimond, P., 2003. Diverse biohopanoid compositions of non-marine sediments. Org. Geochem. 34 (10), 1353–1371.
Ten Haven, H.L., Rohmer, M., Rullkotter, J., Bisseret, P., 1989. Tetrahymanol, the most likely precursor of gammacerane, occurs ubiquitously in marine sediments. Geochim. Cosmochim. Acta 53 (11), 3073.
Tsuzuki, K., Ôhashi, A., Arai, Y., Masuda, K., Takano, A., Shiojima, K., Ageta, H., Cai, S.-Q., 2001. Triterpenoids from *Adiantum caudatum*. Phytochemistry 58 (2), 363–367.
Valentine, J.W., Jablonski, D., 1986. Mass extinctions: sensitivity of marine larval types. PNAS 83 (18), 6912–6914.
van Breugel, Y., Baas, M., Schouten, S., Mattioli, E., Sinninghe Damsté, J.S., 2006. Isorenieratane record in black shales from the Paris Basin, France: constraints on recycling of respired CO2 as a mechanism for negative carbon isotope shifts during the Toarcian oceanic anoxic event. Paleoceanography 21, PA4220.
Veizer, J., Compston, W., 1976. 87Sr/86Sr in Precambrian carbonates as an index of crustal evolution. Geochim. Cosmochim. Acta 40 (8), 905–914.
Visscher, H., Looy, C.V., Collinson, M.E., Brinkhuis, H., van Konijnenburg-van Cittert, J.H.A., Kurschner, W.M., Sephton, M.A., 2004. Environmental mutagenesis during the end-Permian ecological crisis. Proc. Natl. Acad. Sci. U. S. A. 101 (35), 12952–12956.
Volkman, J.K., 1986. A review of sterol markers for marine and terrigenous organic matter. Org. Geochem. 9 (2), 83–99.
Volkman, J., Barrett, S., Blackburn, S., Mansour, M., Sikes, E., Gelin, F., 1998. Microalgal biomakers: a review of recent research developments. Org. Geochem. 29 (5–7), 1163–1180.
Wakeham, S.G., Amann, R., Freeman, K.H., Hopmans, E.C., Jorgensen, B.B., Putnam, I.F., Schouten, S., Sinninghe Damste, J.S., Talbot, H.M., Woebken, D., 2007. Microbial ecology of the stratified water column of the Black Sea as revealed by a comprehensive biomarker study. Organic Geochemistry 38 (12), 2070–2097.
Wang, C., 2007. Anomalous hopane distributions at the Permian–Triassic boundary, Meishan, China – evidence for end-Permian marine ecosystem collapse. Org. Geochem. 38 (1), 52–66.
Wang, C., Visscher, H., 2007. Abundance anomalies of aromatic biomarkers in the Permian–Triassic boundary section at Meishan, China – evidence of end-Permian terrestrial ecosystem collapse. Palaeogeogr. Palaeoclimat. Palaeoecol. 252 (1–2), 291–303.
Wang, C., Lliu, Y., Liu, H., Zhu, L., Shi, Q., 2005. Geochemical significance of the relative enrichment of pristane and the negative excursion of δ^{13}CPr across the Permian–Triassic Boundary at Meishan, China. Chin. Sci. Bull. 50 (19), 2213–2225.
Wang, W., Kano, A., Okumura, T., Ma, Y., Matsumoto, R., Matsuda, N., Ueno, K., Chen, X., Kakuwa, Y., Gharaie, M.H.M., Ilkhchi, M.R., 2007. Isotopic chemostratigraphy of the microbialite-bearing Permian–Triassic boundary section in the Zagros Mountains, Iran. Chem. Geol. 244 (3–4), 708–714.
Watson, J.S., Sephton, M.A., Looy, C.V., Gilmour, I., 2005. Oxygen-containing aromatic compounds in a Late Permian sediment. Org. Geochem. 36 (3), 371–384.
Weidlich, O., Kiessling, W., Flugel, E., 2003. Permian–Triassic boundary interval as a model for forcing marine ecosystem collapse by long-term atmospheric oxygen drop. Geology 31 (11), 961–964.

Wignall, P.B., Twitchett, R.J., 1996. Ocean anoxia and the end Permian mass extinction. Science 272 (5265), 1155–1158.
Wignall, P., Twitchett, R., 2002. Extent, duration and nature of the Permian–Triassic superanoxic event. In: Koeberl, C., MacLeod, K.C. (Eds.), Catastrophic Events and Mass Extinctions: Impacts and Beyond: (Ed. by C. Koeberl, K.C. MacLeod). Geological Society of America Special Paper, vol. 356, pp. 395–413. Boulder, Colorado.
Xie, S., Pancost, R.D., Yin, H., Wang, H., Evershed, R.P., 2005. Two episodes of microbial change coupled with Permo/Triassic faunal mass extinction. Nature 434, 494–497.
Xie, S., Pancost, R.D., Huang, J., Wignall, P.B., Yu, J., Tang, X., Chen, L., Huang, X., Lai, X., 2007. Changes in the global carbon cycle occurred as two episodes during the Permian-Triassic crisis. Geology 35 (12), 1083–1086.
Xu, D.-Y., Yan, Z., 1993. Carbon isotope and iridium event markers near the Permian/Triassic boundary in the Meishan section, Zhejiang Province, China. Palaeogeogr. Palaeoclimat. Palaeoecol. 104 (1–4), 171–176.
Yin, H., Zhang, K., Tong, J., Yang, Z., Wu, S., 2001. The Global Stratotype Section and Point (GSSP) of the Permian–Triassic boundary. Episodes 24 (2), 102–114.
Zhang, K., Tong, J., Yin, H., Wu, S., 1996. Sequence stratigraphy of the Permian–Triassic boundary section of Changxing, Zhejiang. Acta Geol. Sin. 70 (3), 270–281.
Zundel, M., Rohmer, M., 1985a. Hopanoids of the methylotrophic bacteria *Methylococcus capsulatus* and *Methylomonas* sp. as possible precursors of C29 and C30 hopanoid chemical fossils. FEMS Microbiol. Lett. 28, 61–64.
Zundel, M., Rohmer, M., 1985b. Prokaryotic triterpenoids. 1. 3β-Methylhopanoids from *Acetobacter* sp. and *Methylococcus capsulatus*. Eur. J. Biochem. 150, 23–27.